

# PROCEEDINGS OF SPIE

[SPIDigitalLibrary.org/conference-proceedings-of-spie](https://spiedigitallibrary.org/conference-proceedings-of-spie)

## Quantum control in silicon using coherent THz pulses

Stephen A. Lynch, P. Thornton Greenland, Alexander F. G. van der Meer, Benedict N. Murdin, Carl R. Pidgeon, et al.

Stephen A. Lynch, P. Thornton Greenland, Alexander F. G. van der Meer, Benedict N. Murdin, Carl R. Pidgeon, Britta Redlich, Nguyen Q. Vinh, Gabriel Aeppli, "Quantum control in silicon using coherent THz pulses," Proc. SPIE 8496, Terahertz Emitters, Receivers, and Applications III, 84960O (15 October 2012); doi: 10.1117/12.928571

**SPIE.**

Event: SPIE Optical Engineering + Applications, 2012, San Diego, California, United States

# Quantum control in silicon using coherent THz pulses

Stephen A. Lynch<sup>a</sup>, P. Thornton Greenland<sup>b</sup>, Alexander F. G. van der Meer<sup>c</sup>,  
Benedict N. Murdin<sup>d</sup>, Carl R. Pidgeon<sup>e</sup>, Britta Redlich<sup>c</sup>, Nguyen Q. Vinh<sup>f</sup>,  
and Gabriel Aepli<sup>b</sup>

<sup>a</sup>School of Physics and Astronomy, Cardiff University, Queen's Buildings, The Parade,  
CF24 3AA, United Kingdom;

<sup>b</sup>London Centre for Nanotechnology, University College London,  
WC1H 0AH, United Kingdom;

<sup>c</sup>FOM Institute for Plasma Physics "Rijnhuizen", P.O. Box 1207,  
NL-3430 BE, Nieuwegein, The Netherlands;

<sup>d</sup>Advanced Technology Institute, University of Surrey, Guildford,  
GU2 7XH, United Kingdom;

<sup>e</sup>Department of Physics, Heriot-Watt University, Riccarton, Edinburgh,  
EH14 4AS, United Kingdom;

<sup>f</sup>UC Santa Barbara, Institute for Terahertz Science and Technology, Santa Barbara,  
CA 93106-4170, USA

## ABSTRACT

It has long been known that shallow donors such as phosphorous and the other group-V elements, have a hydrogen-like optical spectrum. The main difference is that while the spectrum of atomic hydrogen lies in the visible band, the spectrum of shallow donors in silicon is downshifted to the THz frequency band. This is a direct consequence of the reduced Coulomb attraction seen by the loosely bound electron because the core electrons shield the positive donor atom nucleus, and because the electron is now moving in a dielectric material. While spectroscopy has already revealed much about the energy level structure, very little was known about the temporal dynamics of the system until now. We have used THz pulses from the FELIX free electron laser to probe these hydrogen-like levels. By exploiting the well-known pump-probe technique we have measured the characteristic lifetimes of the excited Rydberg states and found them to be of the order 200 ps. Then, by making subtle changes to the geometry of the pump-probe experimental setup we demonstrate the existence of a THz photon echo. The photon echo is a purely quantum phenomenon with no classical analogue, and it allows us to study the quantum state of the donor electron. We then show, using the photon echo, that it is possible to create a coherent superposition of the ground and excited state of the donor. Measuring the photon echo is important because it can also be used to measure a second important characteristic lifetime of the silicon-donor system, the phase decoherence time.

**Keywords:** Silicon, Quantum Computing, Coherent Control, Shallow Impurities, Rydberg Levels, THz Laser Pulses, Lifetime, Photon Echo

## 1. INTRODUCTION

Crystalline silicon can be conveniently doped by substituting a small number of silicon atoms at lattice sites with atoms from the adjacent pnictogen group-V column of the periodic table. At room temperature this results in an excess of free negative charge carriers and consequently the semiconductor material is termed n-type. At low temperatures, however, the extra electron left over after bonding remains loosely bound to the positive core. This object looks and behaves like an isolated hydrogen atom. There is an analogous Rydberg series of narrow lines in the absorption spectrum but they are shifted towards much lower energies because the Coulomb attraction

---

Further author information: (Send correspondence to S.A.L)

S.A.L.: E-mail: LynchSA@cardiff.ac.uk, Telephone: +44 29 2087 5315

Terahertz Emitters, Receivers, and Applications III, edited by Manijeh Razeghi, Alexei N. Baranov,  
Henry O. Everitt, John M. Zavada, Tariq Manzur, Proc. of SPIE Vol. 8496, 84960O · © 2012 SPIE  
CCC code: 0277-786/12/\$18 · doi: 10.1117/12.928571

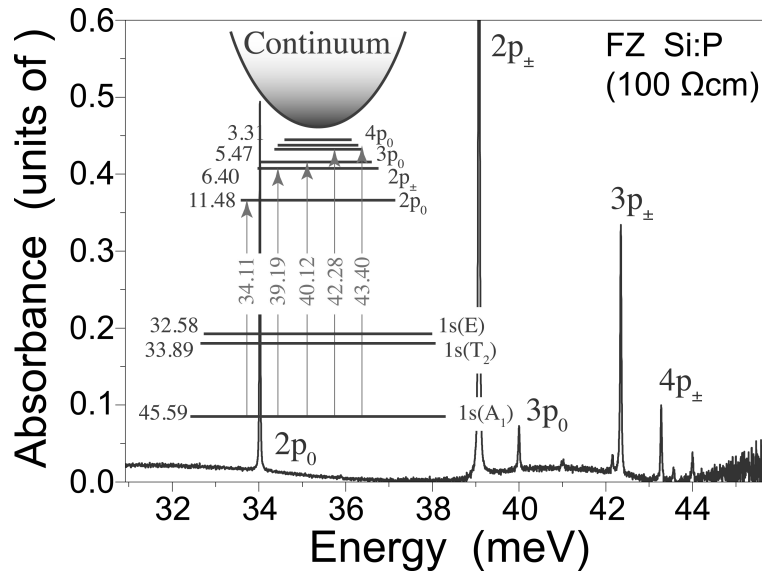


Figure 1. FT-IR absorbance spectrum for a sample of high-resistivity n-type phosphorus doped silicon recorded at 4.2 K. Two Rydberg series of lines,  $np_0$ , and  $np_{\pm}$ , can be clearly observed at meV (THz) energies. The energy level structure has been superimposed over the spectrum in the left hand corner for reference. The Rydberg levels are labelled in to the right of each level, while the relative position of the levels below the conduction band edge are directly to the left of each level. The energies (in meV) of some of the optically allowed transitions observed in the absorbance spectrum are also shown.

between the positive core and the electron is effectively screened by the electrons in the inner shells. The energy separation between these levels now lies in the meV range and thus it can be most conveniently probed with THz radiation. Figure 1 shows a typical Fourier transform infrared (FT-IR) absorbance spectrum for silicon doped with phosphorus measured at 4.2 K. The energy level diagram for the phosphorus donor has been superimposed.

Silicon doped with phosphorus is a particularly interesting material from the point of view of quantum control, and this has led to a dramatic resurgence of activity in the research field. Much of this renewed interest stemmed from a proposal by Kane that silicon doped with group-V donors might be exploited to realise a quantum computer.<sup>1</sup> A related scheme involving group-V donors in silicon was also proposed by Stoneham.<sup>2</sup> The second important development that rekindled interest in this research field was the invention of the optically pumped silicon laser.<sup>3</sup> This breakthrough was the first demonstration of lasing in a silicon-based material, and to-date lasing at THz frequencies has now been demonstrated for all four Group-V donors. Recent work also suggests the possibility of electrically pumped lasing in this material system.<sup>4-6</sup>

A number of experiments designed to investigate the feasibility of Stoneham's quantum computing scheme have now been performed using THz laser light, and are described in this paper. THz pump-probe measurements reveal the lifetimes of the excited states, while THz photon echo experiments show how these states can be manipulated coherently at a quantum level. All of the experiments were performed using the FELIX free electron laser at the FOM institute at Nieuwegein in the Netherlands. The silicon phosphorus lifetime results are discussed in detail in,<sup>7</sup> while full description of the THz pump-probe technique be found in.<sup>8</sup> A full discussion describing the discovery of a THz photon echo can be found in a recent paper.<sup>9</sup> The main cogent points, however, are summarized in this conference paper.

## 2. TERAHERTZ PUMP-PROBE EXPERIMENTS

The pump-probe technique allows temporal phenomenon on a fast time-scale to be studied using a relatively slow THz detector. The basic principle involves exciting electrons into an upper state in the material being probed using a very intense pump pulse, and then monitoring the transmitted intensity of a much weaker probe pulse as the population in the ground state recovers.

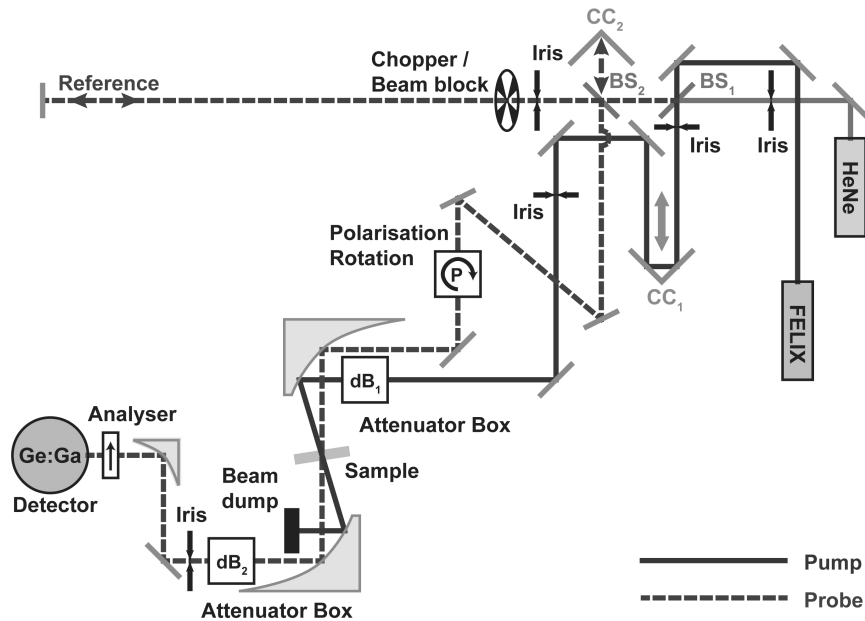


Figure 2. Schematic diagram showing the layout of the pump-probe experimental setup used to measure the lifetimes of the excited donor Rydberg states. A solid line shows the path of the pump beam, while a dashed line shows the path of the probe beam.

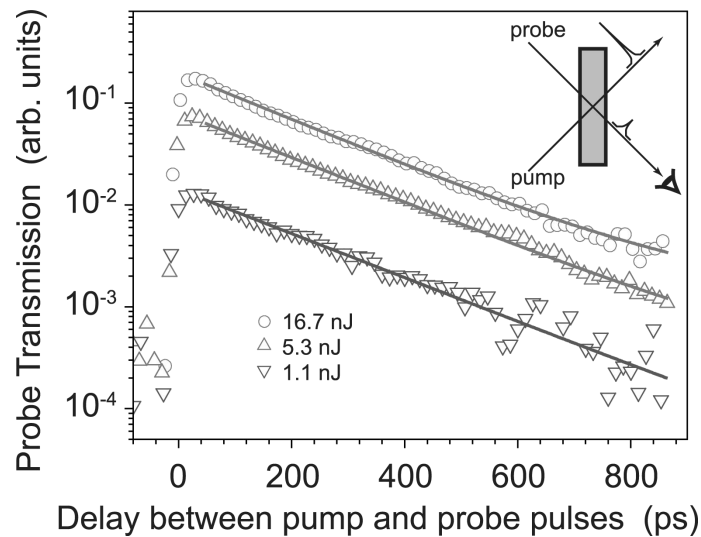


Figure 3. The change in probe transmission induced by the pump as a function of the time delay between pump and probe, observed in the Si:P sample for the  $1s(A_1) \rightarrow 2p_0$  transition at a sample temperature,  $T$ , of 10 K, and a pump and probe photon energy of 34.1 meV. The rise of the leading edge indicates the pulse duration, which was 10 ps. The laser pump powers used correspond to the micropulse energies shown on the figure. The lowest pump pulse energy (1.1 nJ) corresponds to a focused photon fluence of  $10^{17}$  photons/m<sup>2</sup>. Also shown are fits using a single exponential decay where the decay parameter is the spontaneous relaxation rate  $1/T_1$ . (Inset) Transient pump-probe experimental geometry.

We used the free electron laser at the FOM Institute in the Netherlands (FELIX) as a source of short optical (THz) pulses. Figure 2 shows a schematic diagram of the pump-probe experimental setup. The beam path of the stronger pump pulse is shown as a solid line, while the beam path of the weaker probe pulse is shown as a dashed line. The pump traverses an optical delay line, allowing the relative delay between the pump and probe to be controlled. The polarization of the probe is rotated by  $90^\circ$  in order to discriminate it from the pump at the detector. A portion of the probe beam also passes through a much longer optical delay ( $\approx 20$  ns). All beam paths were in a dry nitrogen atmosphere to avoid water vapour absorption. The recorded probe signal is derived from the difference between the directly measured probe and reference signal, resulting in a background free signal. A full description including a diagram of the experimental set-up can be found in.<sup>8</sup>

Figure 3 shows some typical pump-probe transmission data for three different pump pulse energies. Fits to this data with a simple exponential decay gave a value for the lifetime of  $T_1 = 205 \pm 18$  ps. This corresponds to a linewidth of  $1/T_1 = 0.026 \text{ cm}^{-1}$ , that is, less, but not very much less, than the lowest value reported<sup>10</sup> for this transition of  $0.034 \text{ cm}^{-1}$ , which was obtained in an isotopically pure  $^{28}\text{Si}$  sample.

### 3. TERAHERTZ PHOTON ECHO EXPERIMENTS

In order to provide conclusive proof of a true THz photon echo both the directional property and expected timing of the phenomenon need to be established. This is now discussed.

#### 3.1 Echo Direction

The directional property of the echo ( $\mathbf{k}_E = 2\mathbf{k}_2 - \mathbf{k}_1$ ) was established by studying the angular distribution of the beams. In this experiment the pump ( $\mathbf{k}_1$ ) and rephasing ( $\mathbf{k}_2$ ) beams intersect at an angle of  $-5^\circ$ . Simple geometry shows that the echo should emerge at an angle  $+5^\circ$  with respect to the direction of the rephasing beam  $\mathbf{k}_2$ . Figure 5 shows the intensities of the three beams exiting the sample as a function of angle. This graph shows that the echo emerges at the predicted angle with respect to the direction of the rephasing beam  $\mathbf{k}_2$ .

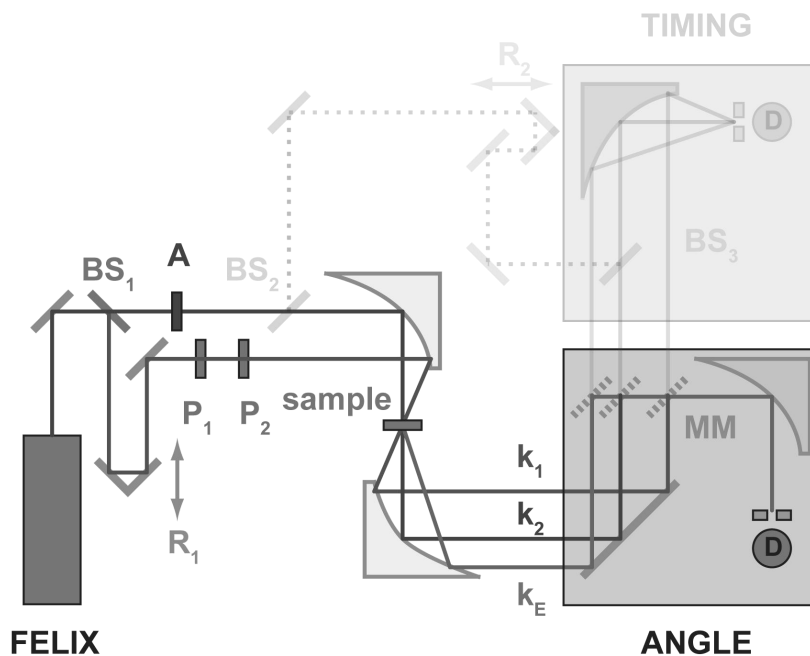


Figure 4. Schematic diagram showing the experimental setup used to determine the angular deflection of the photon echo beam. The modification to this setup used to measure the echo timing in the next section have been purposely faded out to avoid confusion.

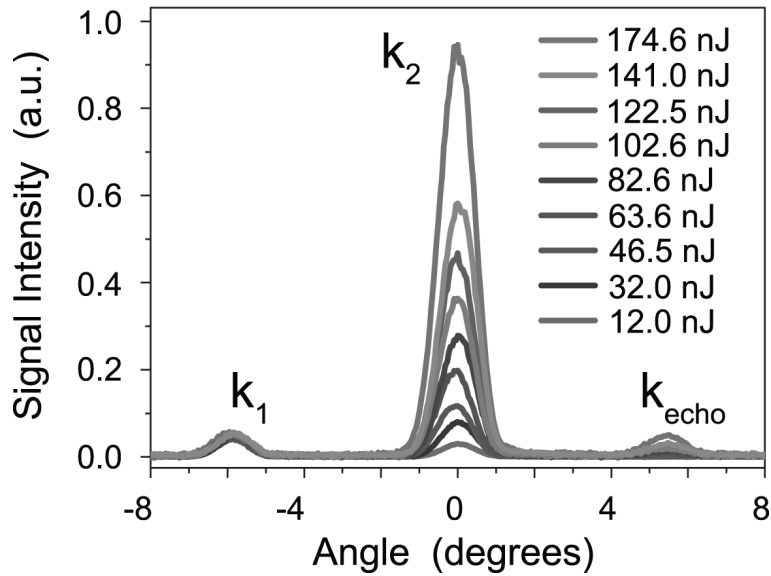


Figure 5. Angle resolved echo. The intensities of the angle resolved signals were recorded by translating the detector across the far-field which shows that ( $k_E = 2k_2 - k_1$ ) as predicted.

### 3.2 Echo Timing

The second important point for consideration is the echo arrival time. This had to be determined indirectly because there are no sufficiently fast detectors in this THz spectral range. A reference pulse was split from the rephasing pulse using a beamsplitter and an extra optical delay line. The transmitted pump, rephasing and emitted echo pulses, as well as the reference pulse are all focussed onto the detector through a pinhole to produce a characteristic interference pattern in time. The angular dispersion of the pump, rephasing and echo pulses is

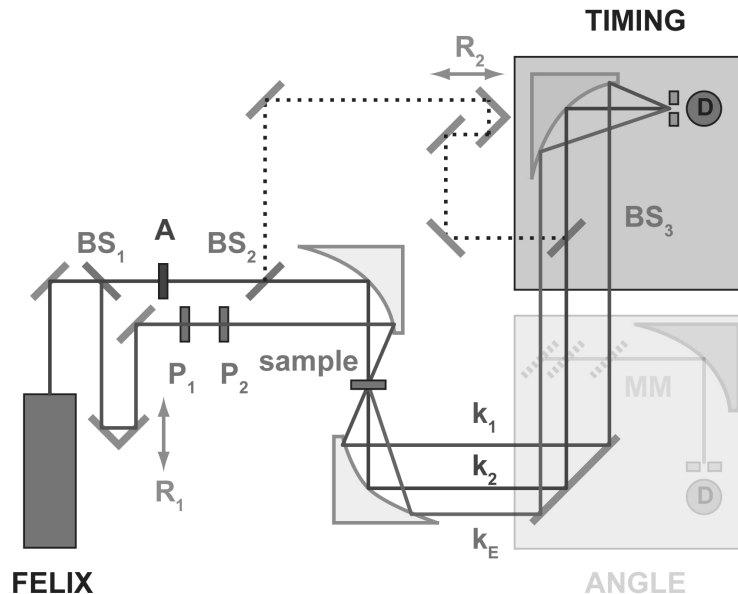


Figure 6. Schematic diagram showing the experimental setup used to determine the timing of the photon echo. The modification to this setup used to measure the echo angle in the previous section have been purposely faded out to avoid confusion.

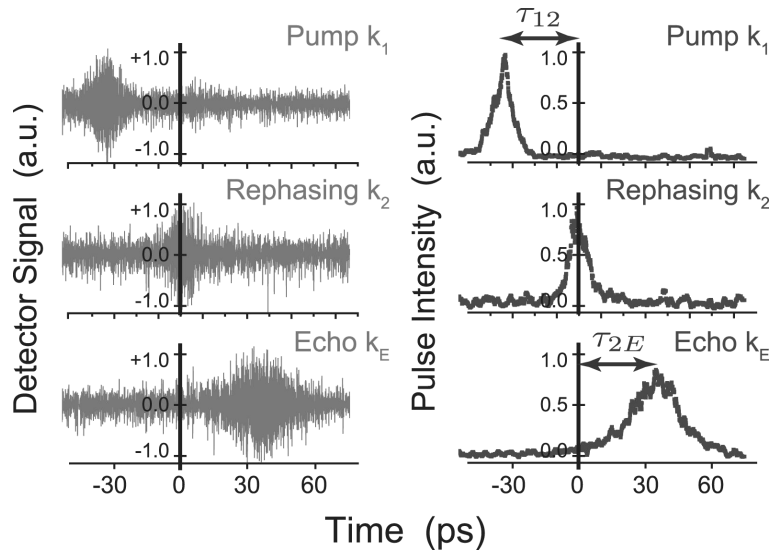


Figure 7. Time resolved echo. On the left is the detector signal showing the interference patterns with the pump, rephasing and echo beams. A moving average has been subtracted, in order to remove the background and laser drift. The pump, rephasing and echo temporal profiles were obtained from the square of these interference patterns, as shown on the right, where the pump rephasing beam time interval  $\tau_{12}$  and the rephasing beam-echo time interval  $\tau_{2E}$  are also shown.

exploited to block all but one of them, thereby obtaining the interference patterns of the reference beam with the pump, rephasing and echo beams separately. By subtracting the mean intensity and squaring the result, the arrival times and shapes of the pump, rephasing and echo pulses can then be determined as a function of time (Figure 7). All three pulses take the form of well-defined peaks, with the maxima occurring at the times anticipated for echoes.

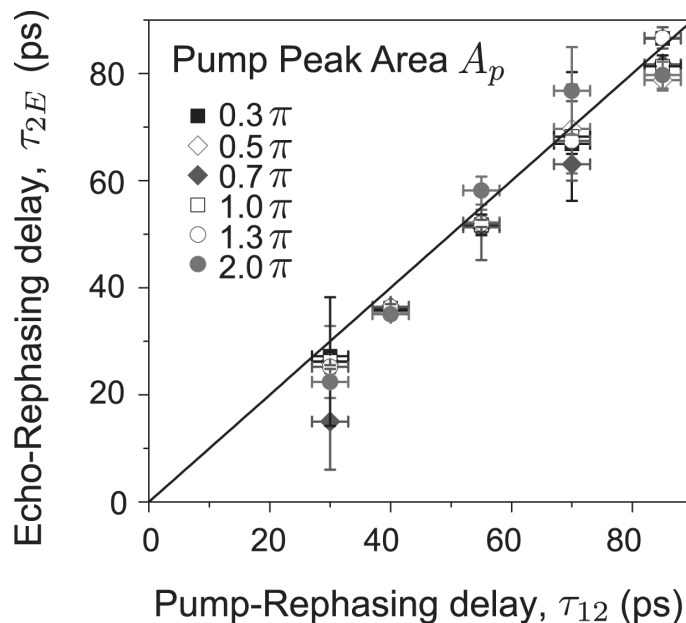


Figure 8. Echo arrival time control. Time resolved cross-correlation experiments, similar to those shown in figure 7, with a range of pump-rephasing delays  $\tau_{12}$ , were used to establish values of the echo delay with respect to the rephasing beam,  $\tau_{2E}$ . Within experimental error, the echo arrives when expected, a finding which is independent of peak pump areas  $A_p$ .

Figure 8 shows a plot of the results of several time resolved cross-correlation experiments, similar to those shown in figure 7. A range of pump-rephasing delays  $\tau_{12}$ , were used to establish values of the echo delay with respect to the rephasing beam,  $\tau_{2E}$ . This figure shows that within experimental error, the echo arrives when expected, a finding which is independent of peak pump areas  $A_P$ . The peak pump area  $A_P$  is defined as the integral of the electric field envelope with respect to time over the duration of the pulse (more simply the product of the square root of the pulse intensity and pulse length).

#### 4. RABI OSCILLATIONS AND COHERENT CONTROL

We now go further to exploit the photon echo as an experimental tool to investigate the quantum coherence properties of the excited donor states. We use the photon echo to directly observe Rabi oscillations produced by coherent optical excitation of phosphorus donors in silicon with intense THz pulses from the free-electron laser. Figure 9 shows the time-integrated photon echo signal  $S$  as a function of pump peak pulse area  $A_P$  for a rephasing peak pulse area of  $0.54\pi$  and a pulse length of 6.79 ps. The dotted line is the ideal theoretical result showing Rabi oscillations. The thin black line shows the corrected prediction when including the non-uniform spatial profile of the laser beam, and the thick grey line includes the effect of both photoionization and the beam profile. The theory lines were calculated using values for  $\mu_{12}$ ,  $\Gamma_0$ ,  $\sigma_{2p0}$  and  $\sigma_e$  that were found from a global fit of many experimental data sets like the one shown here. A full explanation of how this was done can be found in the supplemental information of Greenland's paper.<sup>9</sup> The experimental results for the same conditions are shown as points. The normalisation factor for the ordinate of the experiment relative to the theory was found by a global comparison of many similar experiments with different pulse lengths and rephasing pulse areas. The error bars shown indicate the standard deviation of the normalisation factor (systematic for an individual experiment such the one in this figure) and dominate the statistical errors of the measurements.

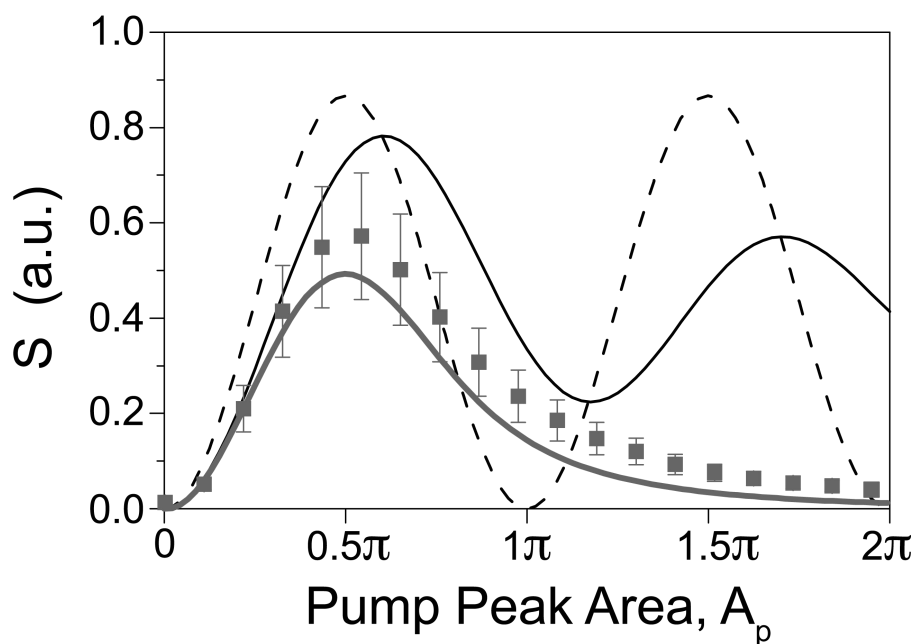


Figure 9. The time-integrated photon echo signal  $S$  as a function of pump peak pulse area  $A_P$  for a rephasing peak pulse area of  $0.54\pi$  and a pulse length of 6.79 ps. The dotted line is the ideal theoretical result showing Rabi oscillations. The thin black line shows the corrected prediction when including the non-uniform spatial profile of the laser beam, and the thick grey line includes the effect of both photoionization and the beam profile. The experimental results for the same conditions are shown as points. The error bars shown indicate the standard deviation of the normalisation factor (systematic for an individual experiment such the one in this figure) and dominate the statistical errors of the measurements.

## 5. CONCLUSION

The THz pump-probe experiments described in this paper in this paper show that the excited phosphor donors are relatively long-lived, certainly long-lived enough to manipulate the superposition of quantum states. Furthermore, the THz photon echo experiments show that coherent mixtures of different orbital states can be prepared on demand. Coherent control of donor orbitals in silicon opens up many possibilities such as entanglement of pairs of impurities whose ground state wavefunctions are too compact to interact. This could ultimately be exploited in a number of silicon-based quantum computing schemes that have been proposed in the literature.

## ACKNOWLEDGMENTS

We acknowledge the financial support of NWO and EPSRC (Advanced Research Fellowship EP/E061265/1 and COMPASSS, Grant Ref EP/H026622/1).

## REFERENCES

1. B. E. Kane, "A silicon-based nuclear spin quantum computer," *Nature* **393**, pp. 133–137, May 1998.
2. A. M. Stoneham, A. J. Fisher, and P. T. Greenland, "Optically driven silicon-based quantum gates with potential for high-temperature operation," *J. Phys. Condens. Matter* **15**, p. L447, July 2003.
3. S. G. Pavlov, R. K. Zhukavin, E. E. Orlova, V. N. Shastin, A. V. Kirsanov, H.-W. Hübers, K. Auen, and H. Riemann, "Stimulated emission from donor transitions in silicon," *Phys. Rev. Lett.* **84**, pp. 5220–5223, May 2000.
4. S. A. Lynch, P. Townsend, G. Matmon, D. J. Paul, M. Bain, H. S. Gamble, J. Zhang, Z. Ikonik, R. W. Kelsall, and P. Harrison, "Temperature dependence of terahertz optical transitions from boron and phosphorus dopant impurities in silicon," *Appl. Phys. Lett.* **87**, p. 101114, September 2005.
5. S. A. Lynch, D. J. Paul, P. Townsend, G. Matmon, Z. Suet, R. W. Kelsall, Z. Ikonik, P. Harrison, J. Zhang, D. J. Norris, A. G. Cullis, C. R. Pidgeon, P. Murzyn, B. N. Murdin, M. Bain, H. S. Gamble, M. Zhao, and W.-X. Ni, "Towards silicon-based lasers for terahertz sources," *IEEE J. Select. Topics Quantum Electron.* **12**, pp. 1570–1578, November/December 2006.
6. S. G. Pavlov, U. Bottger, N. V. Abrosimov, K. Irmscher, H. Riemann, and H.-W. Hübers, "Influence of an electric field on the operation of terahertz intracenter silicon lasers," *J. Appl. Phys.* **107**, p. 033114, February 2010.
7. N. Q. Vinh, P. T. Greenland, K. Litvinenko, B. Redlich, A. F. G. van der Meer, S. A. Lynch, M. Warner, A. M. Stoneham, G. Aeppli, D. J. Paul, C. R. Pidgeon, and B. N. Murdin, "Silicon as a model ion trap: time domain measurements of donor Rydberg states," *Proc. Natl. Acad. Sci. USA* **105**, pp. 10649–10653, August 2008.
8. S. A. Lynch, G. Matmon, S. G. Pavlov, K. L. Litvinenko, B. Redlich, A. F. G. van der Meer, N. V. Abrosimov, and H.-W. Hübers, "Inhomogeneous broadening of phosphorus donor lines in the far-infrared spectra of single-crystalline SiGe," *Phys. Rev. B* **82**, p. 245206, December 2010.
9. P. T. Greenland, S. A. Lynch, A. F. G. van der Meer, B. N. Murdin, C. R. Pidgeon, B. Redlich, N. Q. Vinh, and G. Aeppli, "Coherent control of Rydberg states in silicon," *Nature* **465**, pp. 1057–1061, June 2010.
10. D. Karauskaj, J. A. H. Stotz, T. Meyer, M. L. W. Thewalt, and M. Cardona, "Impurity absorption spectroscopy in  $^{28}\text{Si}$ : the importance of inhomogeneous isotope broadening," *Phys. Rev. Lett.* **90**, pp. 186402–1, May 2003.